GSI

GSI-95-19
PREPRINT
MAERZ 1995

FEW-NEUTRON REMOVAL FROM ^{238}U AT RELATIVISTIC ENERGIES

T. AUMANN, K. SÜMMERER, H. GEISSEL, B. BLANK, T. BROHM, H.-G. CLERC, S. CZAJKOWSKI, C. DONZAUD, A. GREWE, E. HANELT, A. HEINZ, H. IRNICH, M. DE JONG, A. JUNGHANS, J.V. KRATZ, A. MAGEL, G. MÜNZENBERG, F. NICKEL, M. PFÜTZNER, A. PIECHACZEK, C. RÖHL, C. SCHEIDENBERGER, K.-H. SCHMIDT, W. SCHWAB, S. STEINHÄUSER, W. TRINDER, B. VOSS

(Accepted for publication in Z. Phys.)

Gesellschaft für Schwerionenforschung mbH
Postfach 110552 D-64220 Darmstadt Germany

Few-neutron removal from ^{238}U at relativistic energies

T. Aumann[2], K. Sümmerer[1], H. Geissel[1], B. Blank[5], T. Brohm[3], H.-G. Clerc[3], S. Czajkowski[1], C. Donzaud[6], A. Grewe[3], E. Hanelt[3], A. Heinz[3], H. Irnich[1], M. de Jong[3], A. Junghans[3], J.V. Kratz[2], A. Magel[4], G. Münzenberg[1], F. Nickel[1], M. Pfützner[7], A. Piechaczek[1], C. Röhl[3], C. Scheidenberger[1], K.-H. Schmidt[1], W. Schwab[1], S. Steinhäuser[3], W. Trinder[1], and B. Voss[3]

(1) Gesellschaft für Schwerionenforschung mbH, Planckstr. 1, D-64291 Darmstadt, Germany
(2) Institut für Kernchemie, Universität Mainz, Fritz Straßmann-Weg 2, D-55099 Mainz, Germany
(3) Technische Hochschule Darmstadt, Schloßgartenstr. 9, D-64289 Darmstadt, Germany
(4) II. Physikalisches Institut der Universität Giessen, Heinrich-Buff-Ring 16, D-35392 Giessen, Germany
(5) CEN Bordeaux- Gradignan, F-33175 Gradignan, France
(6) IPN, Université de Paris Sud, F-91406 Orsay, France
(7) University of Warsaw, Warsaw, Poland

February 21, 1995

Abstract

As part of a comprehensive study of uranium fragmentation at relativistic energies at the GSI projectile fragment separator, FRS, inclusive neutron-removal cross sections have been measured for several xn channels at projectile energies of 600 and 950 A MeV using targets of Al, Cu and Pb. The variation of the experimental cross sections with target nuclear charge is used to disentangle nuclear and electromagnetic contributions. The electromagnetic cross sections agree surprisingly well with a simple harmonic oscillator calculation of giant dipole resonances based on measured photonuclear cross sections and do not require an extra enhancement of the two-phonon giant dipole excitation as concluded from similar measurements with ^{197}Au.

PACS: 24.30.Cz; 25.75.+r

1 Introduction

The study of multi-phonon giant resonances in nuclei is a topic of current interest both for experimentalists and theorists [1]. The interest is partly related to the fact that large-amplitude vibrations of the neutrons and protons against each other may lead to a considerable instantaneous separation of the proton and neutron densities that could result in the formation of very exotic nuclei when such states decay. The most exciting results can be expected in collisions between the heaviest nuclei at incident energies around 1 A GeV since at these energies the contribution of two-phonon excitations is enhanced relative to single-phonon excitations [2]. Though detailed information on the resonance parameters of multi-phonon giant resonances can only be obtained from exclusive measurements like e.g. those performed at GSI for ^{136}Xe and ^{208}Pb with the LAND neutron detector [3] and for ^{208}Pb with the TAPS γ detector [4], inclusive measurements of few-neutron-removal cross sections can provide complementary information on the cross sections of such resonances and provide constraints for the resonance parameters. First measurements of $1n$ and $2n$ cross sections of target-like ^{197}Au fragments have been published by Hill et al. [5]. Following the same approach, Aumann et al. [6, 7] have shown that the $2n$ and in particular the $3n$ cross sections are very sensitive to the strength of the double giant dipole resonance (DGDR). Recently, fission of ^{238}U at 120 A MeV has been studied [8], but DGDR excitation was not considered by the authors when trying to reproduce the electromagnetic part of the fission cross sections.

The present article reports on $1n$- up to $5n$- removal cross sections for ^{238}U projectiles with energies of 600 and 950 A MeV impinging on ^{27}Al, ^{nat}Cu, and ^{208}Pb targets. The data result from a first comprehensive study of ^{238}U fragmentation performed at the GSI projectile fragment separator FRS [9, 10, 11, 12]. They are complementary to results from an experiment studying target-like fission of ^{238}U induced by ^{208}Pb beams of energies between 100 and 1000 A MeV [13]. We will show below that all our measured xn cross sections can be interpreted consistently under the assumption of a simple harmonic oscillator model of giant resonances, in contrast to the study of neutron-removal from ^{197}Au, where we had to invoke an increased DGDR excitation probability to reproduce the experimental cross sections [6, 7].

2 Experimental Procedure and Results

Beams of ^{238}U accelerated to energies of 600 and 950 A MeV by the GSI heavy-ion synchrotron SIS were directed onto targets of ^{27}Al, ^{nat}Cu, and ^{208}Pb with thicknesses of 377, 205, and 1256 mg/cm^2, respectively. Beam pulses with a spill length of typically 2 s and containing about $5 \cdot 10^6$ ions hit the target approximately every 10 s. Projectile fragments leaving the targets with nearly beam velocity were separated

spatially and identified with respect to nuclear charge and mass, Z and A, with the GSI projectile fragment separator FRS [14]. Since the separation properties of the FRS for uranium fragments have been described in detail in a recent publication [9], we refer the reader to that article and reproduce here only the most pertinent results.

2.1 Separation and identification of neutron-removal products from ^{238}U

A schematic view of the FRS and the associated detectors used to identify the projectile fragments is shown in Fig. 1. Briefly, one- to five-neutron-removal products from the primary ^{238}U beam were identified by measuring their positions in the horizontal plane both in the central (dispersive) and final (achromatic) focal plane of the FRS. As can be seen from Fig. 2, where the xn channels up to ^{234}U are visible, this is sufficient to resolve the different xn channels which emerge from the energy degrader in the central focal plane either fully stripped or after picking up one electron. Two different $B\rho$ settings were sufficient to cover the xn channels up to ^{233}U.

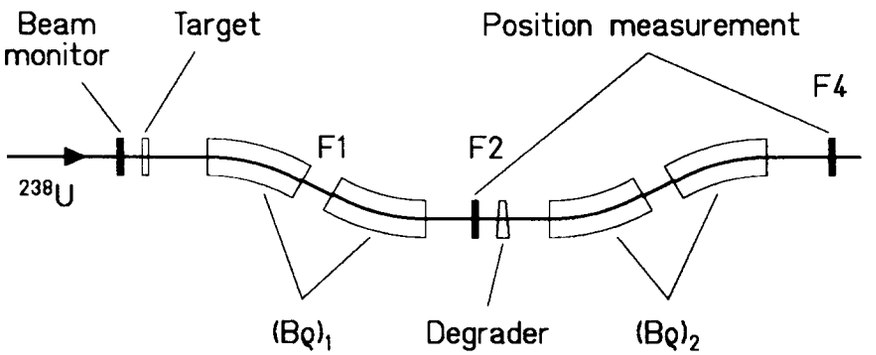

Figure 1: Schematic drawing of the FRS [14]. The fragments were separated and identified according to the $B\rho - \Delta E - B\rho$ separation method [14] by analyzing the magnetic rigidity $(B\rho)_1$ and the atomic energy loss in the degrader with the second dipole stage $((B\rho)_2)$. Two plastic scintillators were used to measure the horizontal positions of the fragments in the central (F2) and final (F4) focal plane of the FRS.

2.2 Calculation of production cross sections

Several corrections have to be applied to calculate formation cross sections for the isotopes $^{233-237}$U from the number of counts observed behind the FRS. The first one is related to the absorption of both projectile and product nuclei in the production target (and in the degrader for the latter). The second correction takes into account

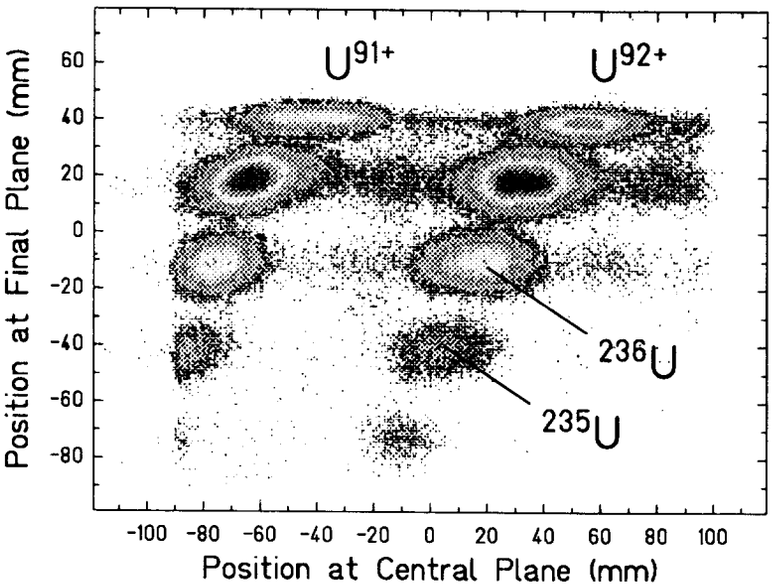

Figure 2: Position distribution of the fragments from a 950 A MeV ^{238}U beam impinging on a ^{208}Pb target, recorded at the central (F2) and final (F4) focal plane of the FRS. The $1n$- to $4n$-removal products are visible either fully stripped (right row) or with charge state $q = 91^+$ (left row) after the degrader. A small fraction of the primary beam that was not completely removed by the slits after the first dipole is also visible.

the population of charge states q other than $q = 92^+$. Note that losses due to different charge states occur both in the production targets and, at a lower average velocity, in the Al degrader and other material in the central plane of the FRS. The charge-state yields behind the targets were measured with the primary beam at the first focal plane F1 [9, 15]. The product of the correction factors describing the losses in the degrader due to reactions and different charge states was measured by transmitting the primary U beam through the FRS. A third correction is necessary due to the finite ion-optical transmission of the FRS, which has been calculated with the Monte-Carlo code MOCADI [16]. The beam intensity has been measured with a secondary-electron-emission detector (SEETRAM, Ref. [17]). For one case, namely the formation of ^{237}U at 950 A MeV, the product of the correction factors described above and the SEETRAM calibration factor could be measured since the $1n$ cross section is so large that ^{237}U could be observed in the final focal plane of the FRS when the primary beam was transmitted for calibration purposes. By comparing to the measurement at higher beam intensity, where the primary beam was cut down by introducing slits behind the first magnet, calibration factors for the beam monitor

were determined. The two values obtained in this way with Cu and Pb targets were found to be in good agreement with each other and were averaged. The resulting SEETRAM calibration factor agree within 10 % with the value obtained by calibrating against a scintillation counter at low intensities [10]. For the measurements at 600 A MeV, the SEETRAM calibration factor was scaled according to the calculated energy loss differences, all other correction factors were derived from data measured with the primary beam.

The resulting experimental cross sections for the formation of the $1n$ to $5n$ products $^{237-233}$U are listed in Col. 3 of Table I for an incident energy of 950 A MeV. Table II lists the $1n$- to $4n$-removal cross sections for an incident energy of 600 A MeV. The same data are visualized in Figs. 3 and 4 for the respective incident energies. For the Pb target the numbers listed have been corrected for multiple reactions in the relatively thick production target, a correction which amounts e.g. to 6 % for the $3n$ cross section.

2.3 Determination of the electromagnetic part of the cross sections

Since at relativistic energies the experimental determination of the impact parameter is difficult, if not impossible, the electromagnetic-dissociation (ED) contribution to the measured xn cross sections can only be obtained by empirically subtracting an estimated nuclear contribution. We estimate nuclear $1n$ cross sections for ^{238}U by starting from the experimental values for the formation of target-like ^{237}U in the reactions of 400 and 1000 A MeV ^{12}C+ ^{238}U, and 1000 A MeV ^{12}Ne+ ^{238}U [18]. Due to the low projectile charge, these cross sections have only a small contribution from ED processes (which has been taken into account, however, in our estimate). The $1n$ cross sections for heavier reaction partners are obtained assuming the same $A^{1/3}$-dependence as in Ref. [6].

For the $2n$ to $5n$ nuclear cross sections, where no other experimental data are available, we base our estimates on our measured total cross sections for the low-Z target ^{27}Al and correct these data for the ED contribution using calculated values. This correction amounts to 60 % and 15 % for the $2n$ an $3n$ channels, respectively, whereas the $4n$ and $5n$ channels are calculated to be of purely nuclear origin. For the $2n$ and $3n$ cases, the $A^{1/3}$-dependence is assumed to be the same as in Ref. [6]. For the $4n$ and $5n$ cases, we assume simply that the ratios of the nuclear cross sections for Pb and Al targets are the same as for the $3n$ channel.

The resulting nuclear cross sections for the different targets are compiled in Col. 5 of Tables I and II and indicated in Figs. 3 and 4 by the long-dashed curves. It is obvious that for the Pb target the $1n$ and $2n$ channels have a nuclear contribution that is of similar size as the experimental error of the data and can therefore be

Table 1: Cross sections for the formation of $1n$- to $5n$-removal products from ^{238}U projectiles at 950 A MeV energy incident on Al, Cu, and Pb targets. The theoretical cross sections are calculated at the average energies in the respective targets.

		Experimental	Calculated cross sections (mb)					
	Target	cross section (mb)	total	nuclear	GDR	DGDR	GQR	ED
$1n$	Al	258±20	262	145	106	0	12	117
$2n$	Al	101±8[a)]	101	43	54	0	4	59
$3n$	Al	25±3[a)]	25	22	2	0	2	4
$4n$	Al	11±2[a)]	11	11	0	0	0	0
$5n$	Al	4.5±0.8[a)]	5	5	0	0	0	0
$1n$	Cu	731±51	676	172	457	0	46	503
$2n$	Cu	288±20	292	47	227	3	15	245
$3n$	Cu	46±4	46	29	6	4	7	17
$4n$	Cu	16±2	17	15	1	1	1	2
$1n$	Pb	2873±201	3029	227	2534	8	260	2802
$2n$	Pb	1122±79	1367	55	1142	88	82	1312
$3n$	Pb	180±15	204	44	26	101	33	160
$4n$	Pb	50±7	46	22	3	19	3	24
$5n$	Pb	12±2	10	9	0	1	0	1

[a)] Cross sections were used to determine nuclear contribution.

Table 2: Same as Table I for $1n$ to $4n$ channels at an incident energy of 600 A MeV.

		Experimental	Calculated cross sections (mb)					
	Target	cross section (mb)	total	nuclear	GDR	DGDR	GQR	ED
$1n$	Al	261±28	253	145	96	0	13	109
$2n$	Al	103±11	92	43	45	0	4	49
$3n$	Al	29±4	25	22	1	0	2	3
$4n$	Al	13±2	11	11	0	0	0	0
$1n$	Cu	646±68	626	172	401	0	52	454
$2n$	Cu	237±25	245	47	180	3	15	198
$3n$	Cu	43±5	43	29	4	4	6	14
$4n$	Cu	15±3	16	15	0	1	0	1
$1n$	Pb	2721±337	2607	227	2082	9	289	2380
$2n$	Pb	932±116	1036	55	820	85	76	981
$3n$	Pb	177±27	166	44	14	82	25	122
$4n$	Pb	59±11	37	22	1	13	2	15

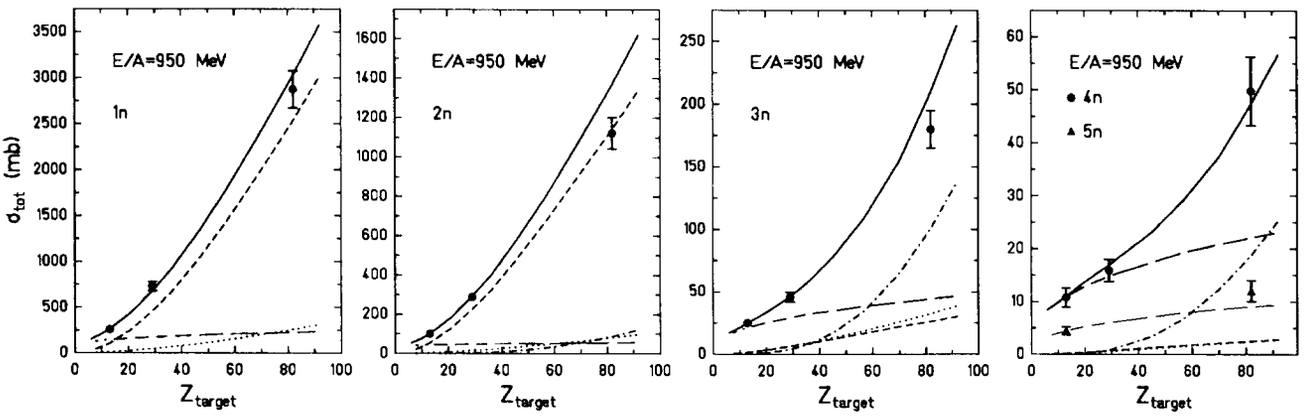

Figure 3: Cross sections for the formation of the $1n$- to $5n$-removal products $^{237-233}$U from ^{238}U projectiles at about 950 A MeV incident on targets with Z_{target}. The full curves indicate our theoretical calculations described in the text. They represent the sum of the nuclear contribution (long-dashed curve), and the electromagnetic contributions due to excitation of the GDR (short-dashed curve), GQR (dotted curve), and DGDR (dot-dashed curve). For the $4n$ channel the dotted curve coincides with the short-dashed one. The triangles and the thin long-dashed curve in the rightmost frame refer to the $5n$ channel.

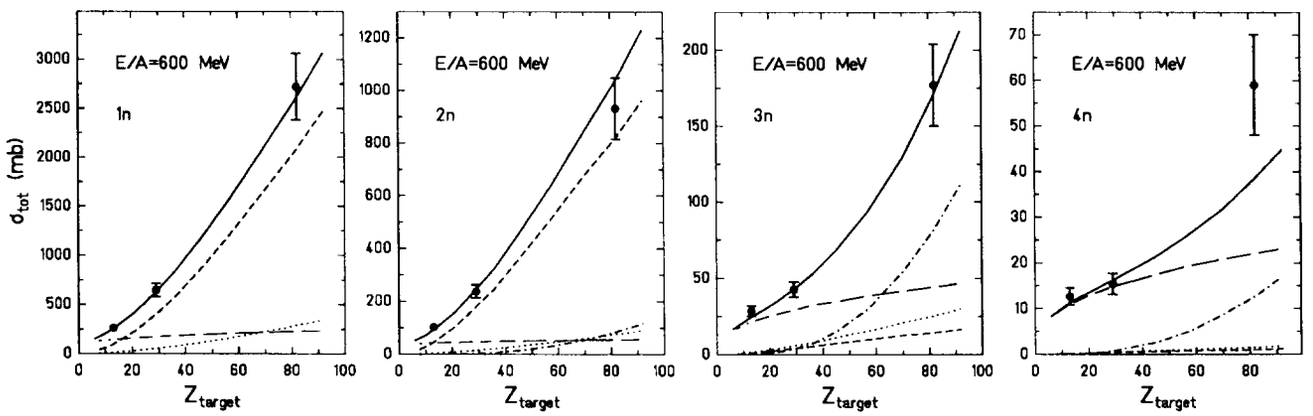

Figure 4: Same as Fig. 1 for $1n$- to $4n$-removal channels, measured at an incident energy of 600 A MeV of the ^{238}U projectiles.

neglected in our discussion. The $3n$ channel has a 25 % contribution from nuclear processes; for the $4n$ channel the 50 % ED contribution is small but visible. It is only the $5n$ channel that is almost exclusively of nuclear origin within our experimental accuracy.

3 Comparison with semi-classical calculations

In the following, we will try to reproduce the ED part of the cross sections of Tables I and II with a semiclassical calculation using empirical parametrizations of the giant dipole (GDR) and giant quadrupole (GQR) resonances. Double-GDR (DGDR) excitations are taken into account using a simple harmonic oscillator model of multiple giant resonances [19, 2]. As elaborated in detail by Aumann et al. [7], this model describes with good accuracy the Z_{proj}-dependence of $1n$-removal cross sections from ^{197}Au targets, but underestimates $3n$-removal from ^{197}Au for Au and Bi projectiles by about 20-30 %. In Ref. [7] it has been shown that the competition between nuclear and electromagnetic processes in near-grazing collisions can be treated properly if one calculates the nuclear transparency with a Glauber-type ansatz using realistic (droplet-model) neutron and proton density distributions. However, calculations with the "sharp-cutoff" approximation (that assumes purely nuclear processes for impact parameters $b < b_{min}$ and purely electromagnetic ones for $b > b_{min}$) have produced almost identical results, if the "BCV" parametrization of b_{min} (Ref. [20]) was used. Thus we feel free to apply the "sharp-cutoff" folding model [7] also in the present study.

The upper part of Fig. 5 shows for 950 A MeV incident energy the differential electromagnetic excitation cross sections for GDR, GQR, and DGDR excitations as calculated with the Lorentzian parameters listed in Table III for the different multipolarities, and by assuming a harmonic model for the DGDR. It should be noted that the Lorentzian parameters for the GDR in ^{238}U determined by the experiments with real photons [21, 22, 23] differ among each other. We have chosen to use the parameters of the most recent experiment (Ref. [23]), but will discuss the consequences of another choice below.

To obtain the final neutron-evaporation cross sections, the neutron-emission probabilities feeding the different xn channels have to be known. Other than in our previous study of ^{197}Au, a calculation of the ED of ^{238}U involves a proper treatment also of the fission deexcitation channel in addition to the neutron-removal channels. Experimentally, photonuclear (γ, n) and (γ, f) cross sections have been measured with real photons up to about 18 MeV excitation energy [21, 23]. However, for our calculations, we need these cross sections up to about 45 MeV, so that a model description is required to calculate them.

For the case of ^{197}Au, we have used the standard evaporation code HIVAP [27]

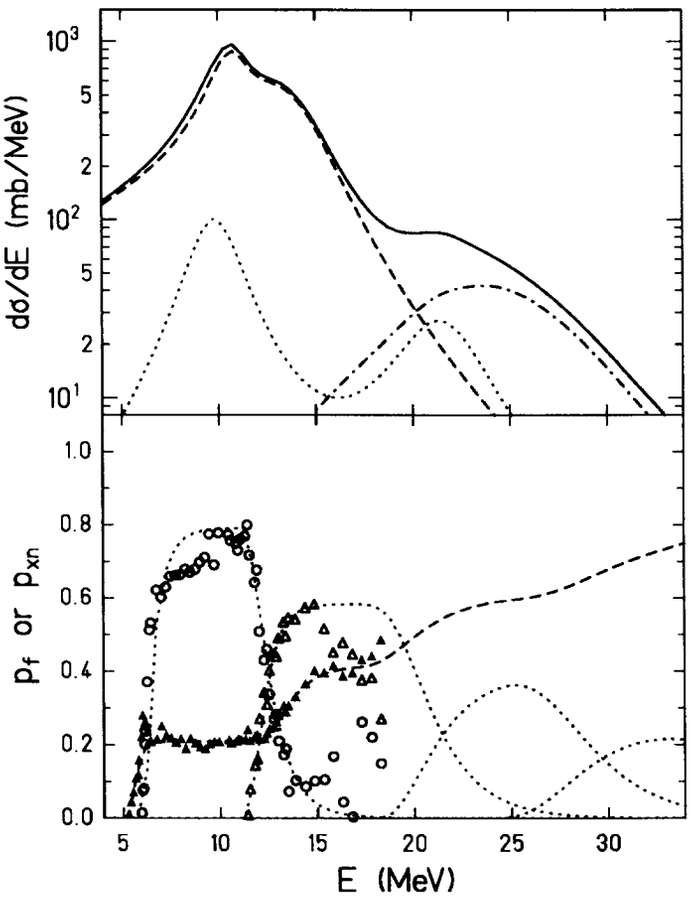

Figure 5: Top: Differential cross sections of GDR (dashed curve), GQR (dotted curve), and DGDR (dot-dashed curve) excitations in ^{238}U as calculated from the equivalent photon spectrum representing a ^{208}Pb nucleus at 920 A MeV, and from parametrizations of the giant resonances in ^{238}U as given in Table III. For the GDR, the Lorentzian parameters of Caldwell et al. [23] have been used. The full line is obtained by summing-up the different contributions. Bottom: Deexcitation probabilities for excited ^{238}U nuclei as a function of excitation energy. The dashed (dotted) curves represent fission (neutron) decay. Filled and open symbols denote measured data for these processes, obtained by dividing the respective partial cross sections from Ref. [23] by the total photoabsorption cross section represented by the Lorentzian parametrization.

Table 3: Parameters of the Lorentzian curves to describe the giant resonances in ^{238}U. For the GDR, two alternative parameter sets by Veyssière et al. [21] and by Caldwell et al. [23] are given.

Resonance	Energy (MeV)	Width (MeV)	Strength (% Sum Rule)	Ref.
GDR	10.96	2.90	41	[21]
	14.04	4.53	78	
GDR	10.77	2.37	34	[23]
	13.80	5.13	109	
GQR(IS)	9.9	3.0	100	[24, 25]
GQR(IV)	21.6	5.0	70	[26]

to calculate the $3n$-emission probability. For the case of ^{238}U, however, we could not reproduce the measured Γ_n/Γ_f-values (see Table IV) with reasonable choices of the model parameters of HIVAP. We therefore decided to use a schematic model developed by Jackson [28] for a reproduction of (p, xn) cross sections that contains the measured Γ_n/Γ_f-values as parameters. In analogy with this prescription, we write for the total fission probability of a ^{238}U nucleus with excitation energy E

$$p_f(E) = f(E)\, p_{1f} \; + \; \sum_{k=2}^{6} p_{kf} \left[1 - e^{-E'(k)/T} \sum_{i=0}^{2k-3} \left(\frac{E'(k)}{T} \right)^i \frac{1}{i!} \right] . \qquad (1)$$

In this equation, p_{kf} denotes the (differential) probability of k^{th} chance fission, which has been measured up to $k = 6$ and is listed in Col. 4 of Table IV. $E'(k)$ is the excitation energy above the threshold for k^{th} chance fission, $E'(k) = E - E_{thr}(k)$, where $E_{thr}(k)$ is the sum of the neutron binding energies of the $(k-1)$ intermediate nuclei and the fission barrier of the nucleus $^{238-k+1}$U, i.e. $E_{thr}(k) = \sum_{i=1}^{k-1} B_n(i) + B_f(k)$. The respective values for these quantities are listed in Cols. 6-8 of Table IV. The parameter T in Eq. 1 is the temperature, $T = \sqrt{\frac{E}{a}}$, with $a = 22 \frac{1}{\text{MeV}}$, whereas $f(E)$ is an exponential function that describes the strong increase of first-chance fission at the barrier, $B_f(1) = 5.7$ MeV, in ^{238}U. We use $f(E) = 1/(1 + exp((B_f - E)/c))$ with $c = 0.6/2\pi$ MeV.

In a similar way, the probability to emit exactly x neutrons, $p_{xn}(E)$, can be written as the difference between the probabilities to emit a minimum of x and $x+1$ neutrons, respectively, $\left(w_{xn}(E) - w_{(x+1)n}(E)\right)$, multiplied by the probability not to undergo fission, $(1 - p_f(E))$, i.e.

$$p_{xn}(E) = \left(w_{xn}(E) - w_{(x+1)n}(E)\right) (1 - p_f(E)) . \qquad (2)$$

Table 4: Parameters used for the calculation of neutron-emission and fission probabilities as described in the text.

k		Γ_n/Γ_f	p_{kf}	p_f	B_n (MeV)	B_f (MeV)	E_{thr} (MeV)
1	^{238}U	3.8[a]	0.21	0.21	6.15[b]	5.7[c]	5.7
2	^{237}U	2.8[a]	0.21	0.42	5.13[b]	6.1[c]	12.3
3	^{236}U	2.1[d]	0.19	0.61	6.55[b]	5.6[c]	16.9
4	^{235}U	1.4[d]	0.17	0.78	5.30[b]	5.9[c]	23.7
5	^{234}U	0.99[d]	0.12	0.90	6.84[b]	5.6[c]	28.7
6	^{233}U	0.49[d]	0.08	0.98	5.76[b]	5.7[e]	35.7

[a]Ref.[23]; [b]Ref.[29]; [c]Ref.[30]; [d]Ref.[31]; [e]Ref.[32].

The probabilities $w_{xn}(E)$ are given by the Jackson formula,

$$w_{xn}(E) = 1 - e^{-E''/T} \sum_{i=0}^{2x-3} \left(\frac{E''(x)}{T}\right)^i \frac{1}{i!}, \tag{3}$$

for $x \geq 2$, with $E''(x)$ now being the excitation energy above the x-neutron-emission threshold, $E'' = E - \sum_{i=1}^{x} B_n(i)$. (Note that $w_{1n} = 1$ above the $1n$-threshold in this description).

In the lower part of Fig. 5 we show the results of these calculations, plotted as a function of the excitation energy of the ^{238}U nucleus. The dotted curves indicate the different xn-evaporation probabilities, Eq. 2, whereas the dashed curve represents the total fission probability, Eq. 1. The agreement with measured (γ, xn) and (γ, f) probabilities from an experiment with real photons [23] is very good below about 15 MeV excitation energy. (A comparison with the results of Ref. [21] shows similar agreement, but is less significant, since this data set does not extend far enough towards low energies). In both cases, however, a marked deviation between measured and calculated p_{1n} values can be noted above 12-15 MeV. This excess cross section has been interpreted as evidence for a direct (non-statistical) $1n$-emission process [21], which is definitely not contained in our statistical neutron-evaporation model. In principle, the proper remedy would be to use directly the measured (γ, xn)-cross sections, which is precluded, however, by the limited statistical accuracy of the high-energy part of the data and by the limited energy range covered. We therefore have to keep in mind that our calculation might overestimate the $2n$ channel by a few percent. The $1n$ and $2n$ channels remain almost unchanged since in case of the $1n$ channel the contribution from direct decay in the excitation-energy region 15-20 MeV is small because of the strongly decreasing photon spectrum. The loss in the $3n$ channel should also be small since the direct decay branch decreases with

increasing energy [33]. Such an uncertainty is tolerable, however, in view of the statistical errors of our data and the uncertainty in the total GDR strength as will be discussed below.

The final inclusive xn-ED cross sections are obtained by multiplying, for each energy interval, the differential excitation cross sections from the upper part of Fig. 5 with the calculated deexcitation probabilities from the lower part and by integrating over excitation energy. The results for the different targets are included in Figs. 3 and 4 (plotted separately for the GDR, GQR, and DGDR contributions). The full curves are obtained by adding up all the ED contributions and the nuclear parts that were calculated as described in Subsection 2.3.

4 Discussion

In our previous study of neutron-removal from ^{197}Au targets (where fission decay after ED could be completely neglected) we could show that the $1n$-removal cross sections could be almost quantitatively reproduced even for large-Z projectiles [6, 7]. For these calculations, we assumed a harmonic oscillator model of the GDR and a minimum impact parameter, b_{min}, according to the BCV parametrization [20].

As can be seen from the left hand parts of Figs. 3 and 4, for the fissile projectile ^{238}U, the same good agreement for the $1n$ channel can be found at both incident energies of 950 and 600 A MeV, respectively. This indicates that the additional degree of freedom of the fission decay channel, which is absent in the ED of ^{197}Au, is correctly taken into account for ^{238}U. An independent corroboration of this fact comes from a direct experimental study of the fission process (which is complementary to neutron emission) by Polikanov et al. [13]. Using ^{208}Pb projectiles of 100, 500, and 1000 A MeV, these authors have determined the ED part of ^{238}U (target) fission. By applying the same parametrization of fission decay after ED as discussed in the present paper, good agreement with the observed ED-fission cross sections has been found [13].

Because of the lower $2n$ threshold for ^{238}U compared to ^{197}Au also the $2n$ cross sections are dominated by single GDR excitation, as can be seen from the middle part of Figs. 3 and 4, and also from Fig. 5. With the exception of the Pb data point taken at 950 A MeV, which is overestimated by about 20 %, also the $2n$ cross sections are well reproduced by the calculation.

It is clear that the agreement between theory and experiment is influenced by the particular choice of the Lorentzian parameters for the GDR in ^{238}U as they are listed in Table III. In particular, it is striking that Caldwell et al. [23] find an integrated GDR strength of 143 % of the energy-weighted sum rule, whereas Veyssière et al. [21] and Gurevich et al. [22] find only 119 % and 123 %, respectively. The latter values seem to be closer to the average percentage found for heavy nuclei [34], nevertheless,

only a comparison with experiment allows to decide which parametrization is more appropriate. For this purpose, we present in Fig. 6 the measured $1n$ to $3n$ cross sections together with calculations performed with the GDR strength from Ref. [23] (full curve) and from Ref. [21] (dashed curve). The figure shows that both parameter sets yield similar agreement with the data; the 600 A MeV data are somewhat closer to the full curve, whereas the 950 A MeV data are better reproduced by the dashed curve. We conclude that only a renewed measurement of the photonuclear cross sections could remove this source of uncertainty in the semiclassical calculations.

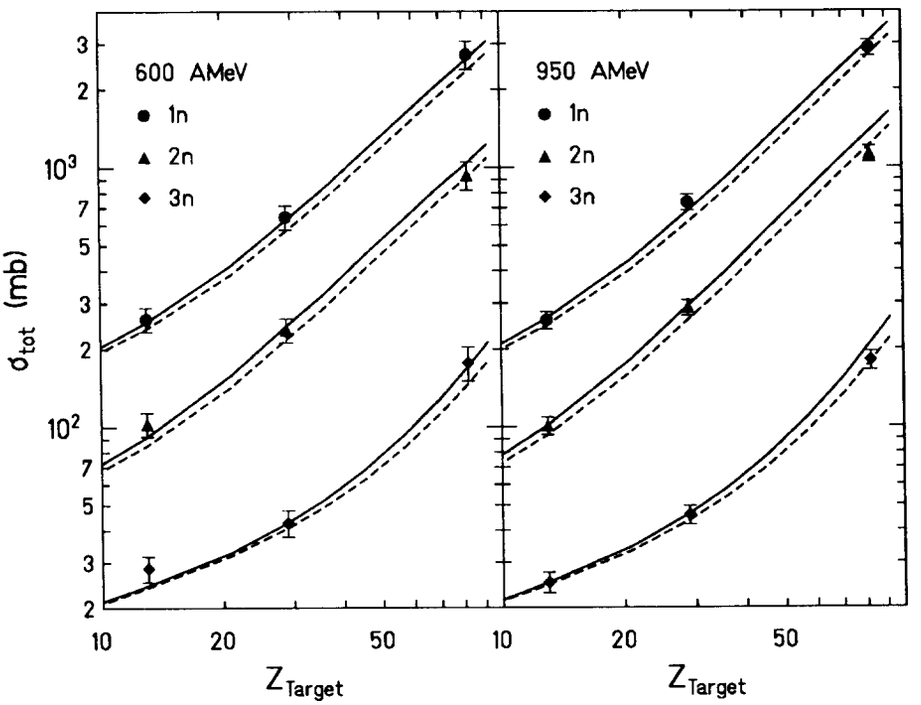

Figure 6: Measured total xn cross sections (including the nuclear part) in comparison with our model calculations using two different experimental values for the integrated GDR strength. The full curve has been drawn with the GDR parameters taken from Caldwell et al. [23], the dashed curve has been obtained using the parameter set from Veyssière et al. [21] (see Table III).

From the decomposition of the individual contributions to the xn cross sections it is obvious that the dominant contribution to the $3n$ cross section for the Pb target is the DGDR. All other processes increase much too slowly with target charge to come even close to the measured data point for the Pb target. The same conclusion can be drawn from the dot-dashed curve in the upper part of Fig. 5, indicating that the DGDR is the dominant process in the excitation energy range between

20 and 30 MeV, where $3n$ emission occurs. When we compare our experimental $3n$ cross sections with the results of our simple calculations, we find that also the $3n$ channels show a similarly good agreement between experiment and theory as the (GDR-dominated) $1n$ and $2n$ channels. This is in contrast with our previous investigation of $3n$ removal from ^{197}Au [6, 7], where we encountered e.g. an excess of about 30 % for the system ^{209}Bi + ^{197}Au [6]. Here, only for the lower energy of 600 A MeV, and only for the GDR parametrization of Veyssière et al., we find an excess of the measured cross section of about 18 % (see left panel in Fig. 6), whereas at 950 A MeV the measured data point coincides exactly with the same calculation. As a further confirmation of our interpretation of measured xn cross sections we note the reasonable agreement also for the $4n$ channel (where the excess from ED comes exclusively from the DGDR, as indicated by the dot-dashed curve) and the absence of any noticeable excess over the nuclear part in the $5n$ channel, as shown by the triangle in the rightmost frame of Fig. 3.

Our calculation of the DGDR cross section involves a folding of the DGDR with itself, implying that the DGDR has exactly twice the energy of the GDR and twice the width. Exclusive measurements have found evidence that the position of the DGDR is rather about 1.9 times the energy of the GDR, and about 20 % narrower than this simple estimate [1]. When we perform our calculation with these modifications, it turns out that they cancel each other almost quantitatively. Taken separately, a shift of the centroid by -1.2 MeV reduces the $3n$ cross section by about 9 mb, whereas a reduction of the width by 20 % alone increases it by about 13 mb.

Thus, we conclude that our simple model used to calculate the DGDR excitation probability is appropriate in the case of ^{238}U, whereas a twice as large DGDR excitation probability was required to reproduce the measured $3n$ cross section in the case of ^{197}Au. We cannot rule out, however, the possibility of an accidental compensation of a larger DGDR excitation probability and a larger fission probability of the same states that are fed by DGDR excitation. (It should be noted that e.g. $3n$ emission occurs only in about one third of all cases with excitation energies in that range, whereas in the other two thirds the nucleus undergoes fission). The direct measurements of the fission cross sections by Polikanov et al. [13] cannot rule out such a possibility since they are sensitive only to the total fission cross section and not to the distribution between different multiphonon excitations: a larger DGDR fission cross section would be more or less compensated by a smaller GDR fission cross section, without producing a net effect that is larger than the uncertainties in their data of about 300 mb.

5 Summary and Conclusions

By measuring formation cross sections of individually resolved isotopes of $^{237-233}$U at the GSI projectile-fragment separator, FRS, the electromagnetic dissociation of ^{238}U could be studied as a function of target nuclear charge and bombarding energy. As in a previous study undertaken with ^{197}Au, the $1n$ channel has been found to be mainly sensitive to the GDR excitation, whereas the $3n$ and $4n$ channels are a sensitive probe of the DGDR excitation. In contrast to the ^{197}Au case, we find no indication that a simple harmonic oscillator model of GDR excitation underestimates the $3n$ cross section by any significant amount. It cannot be ruled out, however, that a larger-than-calculated DGDR cross section manifests itself only in the fission channel. The global trend, however, of electromagnetic neutron-emission and fission cross sections can be well described by our model.

The authors wish to thank the technical staff of the FRS (K.-H. Behr, A. Brünle, K. Burkhard) for their continuous support. We are indebted to H. Folger and the staff of the GSI target laboratory for careful preparation of targets and degraders and to the GSI accelerator crew for providing intense and stable uranium beams.

References

[1] H. Emling, Prog. Part. Nucl. Phys. **33**, 729 (1994).

[2] W.J. Llope and P. Braun-Munzinger, Phys. Rev. C **41**, 2644 (1990); *ibid.* C **45**, 799 (1992).

[3] R. Schmidt, Th. Blaich, Th.W. Elze, H. Emling, H. Freiesleben, K. Grimm, W. Henning, R. Holzmann, J.G. Keller, H. Klingler, R. Kulessa, J.V. Kratz, D. Lambrecht, J.S. Lange, Y. Leifels, E. Lubkiewicz, E.F. Moore, E. Wajda, W. Prokopowicz, Ch. Schütter, H. Spies, K. Stelzer, J. Stroth, W. Walus, H.J. Wollersheim, M. Zinser, and E. Zude, Phys. Rev. Lett. **70**, 1767 (1993); E. Wajda, J. Stroth, Th. Blaich, Th.W. Elze, H. Emling, H. Freiesleben, K. Grimm, W. Henning, R. Holzmann, H. Klingler, R. Kulessa, J.V. Kratz, D. Lambrecht, Y. Leifels, E. Lubkiewicz, E.F. Moore, K. Stelzer, W. Walus, M. Zinser, and E. Zude, Nucl. Phys. **A569**, 141c (1994).

[4] J. Ritman, F.-D. Berg, W. Kühn, V. Metag, R. Novotny, M. Notheisen, P. Paul, M. Pfeiffer, O. Schwalb, H. Löhner, L Venema, A. Gobbi, N. Herrmann, K.D. Hildenbrand, J. Mösner, R.S. Simon, K. Teh, J.P. Wessels und T. Wienold, Phys. Rev. Lett. **70**, 533 (1993); *ibid.* **70** (1993) 2659.

[5] J.C. Hill, F.K. Wohn, J.A. Winger, M. Khayat, M.T. Mercier, and A.R. Smith, Phys. Rev. C **39**, 524 (1989), and references therein.

[6] T. Aumann, J.V. Kratz, E. Stiel, K. Sümmerer, W. Brüchle, M. Schädel, G. Wirth, M. Fauerbach und J.C. Hill, Phys. Rev. C **47**, 1728 (1993); Nucl. Phys. **A569**, 157c (1994) .

[7] T. Aumann, C.A. Bertulani, and K. Sümmerer, Phys. Rev. C **51**, 416 (1995).

[8] M.L. Justice, Y. Blumenfeld, N. Colonna, D.N. Delis, G. Guarino, K. Hanold, J.C. Meng, G.F. Peaslee, G.J. Wozniak, and L.G. Moretto, Phys. Rev. C **49**, R5 (1994).

[9] A. Magel, H. Geissel, B. Voss, P. Armbruster, T. Aumann, M. Bernas, B. Blank, T. Brohm, H.-G. Clerc, S. Czajkowski, H. Folger, A. Grewe, E. Hanelt, A. Heinz, H. Irnich, M. de Jong, A. Junghans, F. Nickel, M. Pfützner, A. Piechaczek, C. Röhl, C. Scheidenberger, K.-H. Schmidt, W. Schwab, S. Steinhäuser, K. Sümmerer, W. Trinder, H. Wollnik, and G. Münzenberg, Nucl. Instr. Meth. in Phys. Res. B **94**, 548 (1994).

[10] H.-G. Clerc, M. de Jong, T. Brohm, M. Dornik, A. Grewe, E. Hanelt, A. Heinz, A. Junghans, C. Röhl, S. Steinhäuser, B. Voss, C. Ziegler, K.-H. Schmidt, S. Czajkowski, H. Geissel, H. Irnich, A. Magel, G. Münzenberg, F. Nickel,

A. Piechaczek, C. Scheidenberger, W. Schwab, K. Sümmerer, W. Trinder, M. Pfützner, B. Blank, A. Ignatyuk, and G. Kudyaev, Preprint IKDA 94/17, submitted to Nucl. Phys..

[11] K.-H. Schmidt, A. Heinz, H.-G. Clerc, B. Blank, T. Brohm, S. Czajkowski, C. Donzaud, H. Geissel, E. Hanelt, H. Irnich, M.C. Itkis, M. de Jong, A. Junghans, A. Magel, G. Münzenberg, F. Nickel, M. Pfützner, A. Piechaczek, C. Röhl, C. Scheidenberger, W. Schwab, S. Steinhäuser, K. Sümmerer, W. Trinder, B. Voss, and S.V. Zhdanov, Phys. Lett. **B 325**, 313 (1994).

[12] M. Hesse, M. Bernas, P. Armbruster, H. Geissel, T. Aumann, S. Czajkowski, Ph. Dessagne, C. Donzaud, E. Hanelt, A. Heinz, C. Kozhuharov, Ch. Miehe, G. Münzenberg, C. Röhl, K.-H. Schmidt, W. Schwab, C. Stéphan, K. Sümmerer, and L. Tassan-Got, to be submitted to Z. Phys.

[13] S. Polikanov, W.Brüchle, H. Folger, E. Jäger, T. Krogulski, M. Schädel, E. Schimpf, G. Wirth, T. Aumann, J.V. Kratz, E. Stiel, and N. Trautmann, Z. Phys. A **350**, 221 (1994).

[14] H. Geissel, P. Armbruster, K.H. Behr, A. Brünle, K. Burkard, M. Chen, H. Folger, B. Franczak, H. Keller, O. Klepper, B. Langenbeck, F. Nickel, E. Pfeng, M. Pfützner, E. Roeckl, K. Rykaczewski, I. Schall, D. Schardt, C. Scheidenberger, K.-H. Schmidt, A. Schröter, T. Schwab, K. Sümmerer, M. Weber, G. Münzenberg, T. Brohm, H.-G. Clerc, M. Fauerbach, J.-J. Gaimard, A. Grewe, E. Hanelt, B. Knödler, M. Steiner, B. Voss, J. Weckenmann, C. Ziegler, A. Magel, H. Wollnik, J.P. Dufour, Y. Fujita, D.J. Vieira, and B. Sherrill, Nucl. Instr. Meth. in Phys. Res. B **70**, 286 (1992).

[15] C. Scheidenberger, H. Geissel, Th. Stöhlker, H. Folger, H. Irnich, C. Kozhuharov, A. Magel, P.H. Mokler, R. Moshammer, G. Münzenberg, F. Nickel, M. Pfützner, P. Rymuza, W. Schwab, J. Ullrich, and B. Voss, Nucl. Instr. Meth. in Phys. Res. B **90**, 36 (1994).

[16] T. Schwab, Ph.D. thesis, GSI Report, GSI-91-10 (1991), ISSN 0171-4546.

[17] C. Ziegler, T. Brohm, H.-G. Clerc, H. Geissel, K.-H. Schmidt, K. Sümmerer, D. Vieira, and B. Voss, GSI scientific report 1990, GSI-91-1, p.291 (1991).

[18] P.L. McGaughey, W. Loveland, D.J. Morrissey, K. Aleklett, and G.T. Seaborg, Phys. Rev. C **31**, 896 (1985).

[19] C.A. Bertulani and G. Baur, Phys. Reports **163**, 299 (1988).

[20] C.J. Benesh, B.C. Cook, and J.P. Vary, Phys. Rev. C **40**, 1198 (1989).

[21] A. Veyssière, H. Beil, R. Bergère, P. Carlos, A. Leprêtre, and K. Kernbath, Nucl. Phys. **A199**, 45 (1973).

[22] G.M. Gurevich, L.E. Lazareva, V.M. Mazur, G.V. Solodokhov, and B.A. Tulupov, Nucl. Phys. **A273**, 326 (1976).

[23] J.T. Caldwell, E.J. Dowdy, B.L. Berman, R.A. Alvarez, and P. Meyer, Phys. Rev. C **21**, 1215 (1980).

[24] Th. Weber, R.D. Heil, U. Kneissl, W. Pecho, W. Wilke, Th. Kihm, K.T. Knöpfle, and H.J. Emrich, Nucl. Phys. **A510**, 1 (1990).

[25] F. Gerab and M.N. Martins, Phys Rev. C **48**, 105 (1993).

[26] R. Pitthan, F.R. Buskirk, W.A. Houk, and R.W. Moore, Phys. Rev. C **21**, 28 (1980).

[27] GSI version of the code ALICE (M. Blann and F. Plasil, Phys. Rev. Lett. **29** (1972) 303); W. Reisdorf and M. Schädel, Z. Phys. A **343** (1992) 47.

[28] J.D. Jackson, Can. J. Phys. **34**, 767 (1956), cited in: J.G. Keller, Diploma Thesis, TH Darmstadt, (1981).

[29] G. Audi and A.H. Wapstra, Nucl. Phys. **A565**, 1 (1993).

[30] C. Wagemans, *The Nuclear Fission Process*, CRC Press (1991).

[31] B.L. Berman, R.E. Pywell, S.S. Dietrich, M.N. Thompson, K.G. McNeill, and J.W. Jury, Phys. Rev. C **34**, 2201 (1986).

[32] R. Vandenbosch and J.R. Huizenga, *Nuclear Fission*, Academic Press (1973).

[33] A. van der Woude, D. Chmielewska, A.M. van den Berg, Y. Blumenfeld, N. Alamanos, F. Auger, J. Blomgren, J. Bordewijk, S. Brandenburg, N. Frascaria, A. Gillibert, L. Nilsson, N. Olsson, P. Roussel-Chomaz, J.C. Roynette, J.A. Scarpaci, T. Suomijärvi, and R. Turcotte, Nucl. Phys. **A569**, 383c (1994).

[34] S.S. Dietrich and B.L. Berman, At. Data and Nucl. Data Tables **38**, 199 (1988).